# A Wire-Based Active Tracker

Juan Andrade-Cetto and Federico Thomas

*Abstract*— Wire-based tracking devices are an affordable alternative to costly tracking devices. They consist of a fixed base and a platform, attached to the moving object, connected by six wires whose tension is maintained along the tracked trajectory. One important shortcoming of this kind of devices is that they are forced to operate in reduced workspaces so as to avoid singular configurations. Singularities can be eliminated by adding more wires but this causes more wire interferences, and a higher force exerted on the moving object by the measuring device itself. This paper shows how, by introducing a rotating base, the number of wires can be reduced to three, and singularities can be avoided by using an active sensing strategy. This also permits reducing wire interference problems and the pulling force exerted by the device.

*Index Terms*— Tracking devices, active sensing, mutual information, parallel manipulators, Kalman filtering.

## I. INTRODUCTION

**T**RACKING devices are used for estimating the position and orientation of moving objects, and are often based on electromagnetic, acoustic, mechanical, or optical technology. Tracking devices can be classified according to their characteristics, such as accuracy, resolution, cost, measurement range, portability, and calibration requirements. Laser tracking systems exhibit good accuracy, which can be less than $1\mu m$ if the system is well calibrated. Unfortunately, this kind of systems are very expensive, their calibration procedure is time-consuming, and they are sensitive to the environment. Vision systems can reach an accuracy of $0.1mm$. They are low-cost portable devices but their calibration procedure can be complicated. Wire-based systems can reach an accuracy of $0.1mm$, they are also low cost portable devices but capable of measuring large displacements. Moreover, they exhibit a good compromise among accuracy, measurement range, cost and operability.

Wire-based tracking devices consist of a fixed base and a platform connected by six wires whose tension is maintained, while the platform is moved, by pulleys and spiral springs on the base, where a set of encoders give the length of the wires. They can be modelled as 6-DOF parallel manipulators because wires can be seen as extensible legs connecting the platform and the base by means of spherical and universal joints, respectively.

Dimension deviations due to fabrication tolerances, wire-length uncertainties, or wire slackness, may result in un-
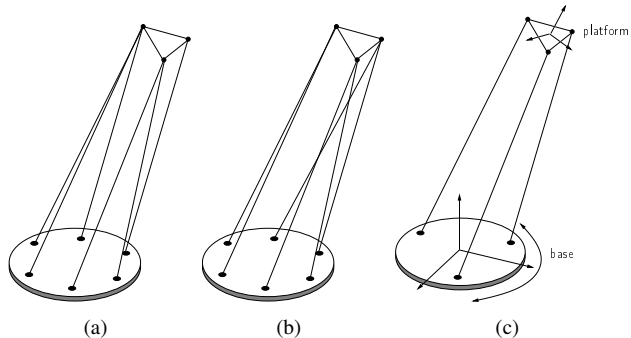
Fig. 1. Different configurations of wire-based tracking devices: (a) the "3-2-1" configuration, (b) the "2-2-2" configuration, and (c) the proposed tracking device.

acceptable performance of a wire-based tracking device. In general, the effects of all systematic errors can be eliminated by calibration. Some techniques to calibrate for specific errors have already been proposed in the literature. For example, a method for compensating the cable guide outlet shape of wire encoders is detailed in [1], and a method for compensating the deflections caused by wire self-weights is described in [2]. In this paper, we will only consider wire-length errors which cannot be compensated because of their random nature.

Another indirect source of error is the force exerted by the measuring device itself. Indeed, all commercial wire encoders are designed to keep a large string tension. This is necessary to ensure that the inertia of the mechanism does not result in a wire going slack during a rapid motion. If a low wire force is used, it would reduce the maximum speed of the object to be tracked without the wires going slack. On the contrary, if a high wire force is used, the trajectory of the object to be tracked could be altered by the measuring device. Hence, a trade-off between accuracy and speed arises.

The minimum number of points on a moving object to be tracked for pose measurements is three. Moreover, the maximum number of wires attached to a point is also three, otherwise the lengths of the wires will not be independent. This leads to only two possible configurations for the attachments on the moving object. The *3-2-1 configuration* was proposed in [1]. The kinematics of this configuration was studied, for example, in [3] and [4]. Its direct kinematics can be solved in closed-form by using three consecutive trilateration operations yielding 8 solutions, as in [5]. The *2-2-2 configuration* was first proposed in [2] for a wire-based tracking device. The kinematics of this configuration was studied, for example, in [6], [7], and [8] where it was shown that its forward kinematics has 16 solutions. In other words, there are up to 16 poses for the moving object compatible with a given set of wire lengths. These configurations can only be obtained by a numerical method. The two configurations

above were compared, in terms of their sensitivity to wire-length errors, in [1]. The conclusion was that they have similar properties.

In order to reduce cable interferences, singularities, and wire tension problems we choose to reduce the number of cables from six to three, and to have the base rotate on its center (see Figure 1). Provided that the tracked object motion is sufficiently slow, two measurements at different base orientations would be equivalent to a 2-2-2 configuration. More elegantly, and to let the tracked object move at faster speeds, measurements can be integrated sequentially through a partially observable estimation framework.

The remainder of the paper is organized as follows. Section 2 contains the kinematics model of our proposed 3-wire-based sensing device; Section 3 describes the filtering strategy for pose tracking. Given that this device has a moving part, Section 4 develops an information theoretic metric for choosing the best actions for controlling it. A strategy to prevent possible wire crossings is contemplated in Section 5. Section 6 is devoted to a set of examples demonstrating the viability of the proposed approach. Finally, concluding remarks are presented in Section 7.

## II. KINEMATICS OF THE PROPOSED SENSOR

Consider the 3-wire parallel device in Figure 1(c). It is assumed that the platform configuration is free to move in any direction in $\mathbb{R}^3 \times SO(3)$. Let the state of our tracking device be defined as the 12-dimensional array

$$\mathbf{x} = \begin{bmatrix} \mathbf{p} \\ \boldsymbol{\theta} \\ \mathbf{v} \\ \boldsymbol{\omega} \end{bmatrix} , \qquad (1)$$

where $\mathbf{p} = (x, y, z)^\top$ is the position of the origin of a coordinate frame fixed to the platform, $\boldsymbol{\theta} = (\psi, \theta, \phi)^\top$ is the orientation of such coordinate frame expressed as yaw, pitch and roll angles, and $\mathbf{v} = (v_x, v_y, v_z)^\top$ and $\boldsymbol{\omega} = (\omega_x, \omega_y, \omega_z)^\top$ are the translational and rotational velocities of $\mathbf{p}$, respectively.

Assume that the attaching points on the base $\mathbf{a}_i$, $i = 1, 2, 3$, are distributed on a circle of radius $\bar{a}$ as shown in Figure 2. Then, the coordinates of $\mathbf{a}_i$ can be expressed in terms of the base rotation angle $\beta$ as

$$\begin{bmatrix} a_{xi} \\ a_{yi} \\ a_{zi} \end{bmatrix} = \begin{bmatrix} \bar{a}\cos(\beta + \rho_i) \\ \bar{a}\sin(\beta + \rho_i) \\ 0 \end{bmatrix} . \qquad (2)$$

Moreover, let $\mathbf{e}_i$ be the unit norm vector specifying the direction from $\mathbf{a}_i$ to the corresponding attaching point $\mathbf{b}_i$ in the platform; and let $l_i$ be the length of the $i$-th wire. The position of the wire attaching points in the platform, in global coordinates, are

$$\mathbf{b}_i = \mathbf{a}_i + l_i \mathbf{e}_i = \mathbf{p} + R\bar{\mathbf{b}}_i . \qquad (3)$$

The value of $\bar{\mathbf{b}}_i$ is constant and is expressed in platform local coordinates, and $R$ is the rotation matrix describing the orientation of the platform.
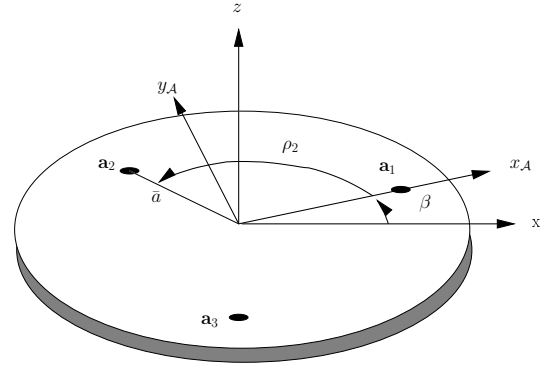


Fig. 2.    The rotating base.

## III. STATE ESTIMATION

The objective is to track the platfrom motion from wire length measurements. And to do it, we adopt a smooth unconstrained constant-velocity model for the motion of the platform, its pose altered only by zero-mean, normally distributed accelerations. The Gaussian acceleration assumption means that large impulsive changes of direction are unlikely. In such model, the prediction of the position and orientation of the platform at time $t$ plus a time interval $\tau$ is given by

$$\begin{bmatrix} \mathbf{p}(t+\tau) \\ \boldsymbol{\theta}(t+\tau) \end{bmatrix} = \begin{bmatrix} \mathbf{p}(t) + \mathbf{v}(t)\tau + \boldsymbol{\delta}_a(t)\tau^2/2 \\ \boldsymbol{\theta}(t) + \boldsymbol{\omega}(t)\tau + \boldsymbol{\delta}_\alpha(t)\tau^2/2 \end{bmatrix} , \qquad (4)$$

with $\boldsymbol{\delta}_x = (\boldsymbol{\delta}_a, \boldsymbol{\delta}_\alpha)$ zero mean white Gaussian translational and angular acceleration noises. Moreover, the adopted model for the translational and angular velocities of the platform is given by

$$\begin{bmatrix} \mathbf{v}(t+\tau) \\ \boldsymbol{\omega}(t+\tau) \end{bmatrix} = \begin{bmatrix} \mathbf{v}(t) + \boldsymbol{\delta}_a(t)\tau \\ \boldsymbol{\omega}(t) + \boldsymbol{\delta}_\alpha(t)\tau \end{bmatrix} . \qquad (5)$$

In practice, measured wire lengths will be corrupted by some sources of uncertainty (i.e., wire tension variations) which will be modelled as additive Gaussian noise, $\boldsymbol{\delta}_{z_i}$. The kinematics relation fo platform pose and wire lengths is

$$z_i(t) = l_i(t) + \boldsymbol{\delta}_{z_i}(t) = \|\mathbf{p}(t) + R(t)\bar{\mathbf{b}}_i - \mathbf{a}_i(t)\| + \boldsymbol{\delta}_{z_i}(t) . \qquad (6)$$

An Extended Kalman Filter can be used to propagate the platform pose and velocity estimates, as well as the base orientation estimates, and then, to refine these estimates through wire length measurements. To this end, $\boldsymbol{\delta}_x \sim N(\mathbf{0}, \Sigma_x)$, $\boldsymbol{\delta}_{z_i} \sim N(\mathbf{0}, \Sigma_{z_i})$, the motion model $\mathbf{f}(\mathbf{x}, \boldsymbol{\delta}_x)$ is given in Eqs. (4) and (5), the measurement model is $\mathbf{h}(\mathbf{x}, \boldsymbol{\delta}_{z_i})$ from Eq. (6), and the plant Jacobians with respect to the state and to the noise become

$$F = \frac{\partial \mathbf{f}}{\partial \mathbf{x}} = \begin{bmatrix} I & \tau I \\ 0 & I \end{bmatrix} \qquad (7)$$

and

$$G = \frac{\partial \mathbf{f}}{\partial \boldsymbol{\delta}_x} = \begin{bmatrix} \frac{\tau^2 I}{2} \\ \tau I \end{bmatrix} . \qquad (8)$$

The measurement Jacobians are simply

$$H_i(t) = \frac{\partial \mathbf{h}_i}{\partial \mathbf{x}} = \begin{bmatrix} \mathbf{e}_i(t)^\top & (\bar{\mathbf{b}}_i \times \mathbf{e}_i(t))^\top & \mathbf{0}_{1\times 6} \end{bmatrix} , \qquad (9)$$
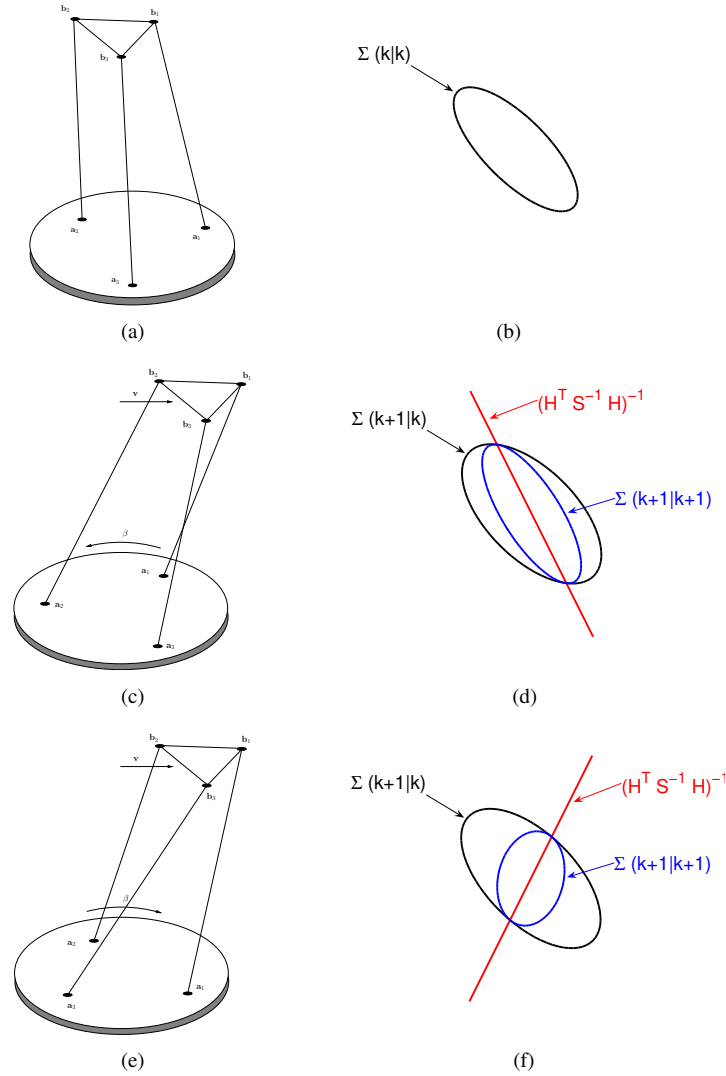
Fig. 3. Active sensing strategy. Frame (a) exemplifies one possible sensor configuration. The platform is expected to move at constant velocity, indicated by the vector $\mathbf{v}$. Two choices for rotating the base need be analyzed, counterclockwise (frame c), and clockwise (frame e). Each base rotation command would induce an expected growth in the estimated platform position uncertainty, from the covariance hyperellipsoid $\Sigma(k|k)$ shown in (b) to the larger covariance hyperellipsoids $\Sigma(k+1|k)$ in frames (d) and (f). Expected measurements from the two different configurations would reduce the estimated platform position uncertainty by different amounts, depending on the orientation of the degenerate wire contribution $(H^\top S^{-1} H)^{-1}$ with respect to the platform pose uncertainty. The command chosen is the one for which relative entropy is minimized, and in this particular case, that of frames (e) and (f).

with

$$\mathbf{e}_i(t) = \frac{\mathbf{p}(t) + R(t)\bar{\mathbf{b}}_i - \mathbf{a}_i(t)}{\|\mathbf{p}(t) + R(t)\bar{\mathbf{b}}_i - \mathbf{a}_i(t)\|} \ . \tag{10}$$

For the sake of clarity, in the sequel, and when needed, time dependencies $t + \tau|t$ will be used to indicate prior estimates (before measurements are incorporated), and the terms $t|t$ and $t + \tau|t + \tau$ will represent posterior estimates (once measurements are taken into account). The prediction of the state and state covariance are given by

$$\mathbf{x}(t + \tau|t) = \mathbf{f}(\mathbf{x}(t|t), \mathbf{0}) \tag{11}$$

$$\Sigma(t + \tau|t) = F\Sigma(t|t)F^\top + G\Sigma_x G^\top \tag{12}$$

and, the revision of the state estimate and state covariance are

$$\mathbf{x}(t + \tau, t + \tau) = \mathbf{x}(t + \tau|t) + K(\mathbf{z}(t + \tau) - \mathbf{h}(\mathbf{x}(t + \tau|t), \mathbf{0})) \tag{13}$$

$$\Sigma(t + \tau|t + \tau) = (I - KH)\Sigma(t + \tau|t) \tag{14}$$

with $K = \Sigma(t + \tau|t)H^\top(H\Sigma(t + \tau|t)H^\top + \Sigma_z)^{-1}$ the usual Kalman gain.

Given that our estimation scheme is partially observable, wire lenght measurements can be used to revise state estimates along a 3-dimensional subspace of the state space only. The information gained from measuring only three wires at a time is $H^\top(H\Sigma(t + \tau|t)H^\top + \Sigma_z)^{-1}H$, and it is singular. The unobservable directions in state space are indicated by the null space of this matrix, whereas the directions in state space for which uncertainty can be reduced from these measurements are orthogonal to that null space. The control strategy described next will allow us to choose the best base rotation commands for reducing overall platform pose uncertainty from partial measurements.

## IV. Control Strategy

In this Section we develop a control strategy for rotating the base of our proposed 3-wire sensor structure. The aim is to rotate the base in the direction that most reduces the uncertainty in the entire pose state estimate, by using the information that should be *gained* from future wire measurements were such a move be made.

The essential idea is to use mutual information as a measure of the statistical dependence between the platform pose and the wire lengths. The mutual information is the relative entropy between the marginal density $p(\mathbf{x})$ and the conditional $p(\mathbf{x}|\mathbf{z})$

$$\mathcal{I}(\mathbf{x}, \mathbf{z}) = \int_{\mathbf{x},\mathbf{z}} p(\mathbf{x}, \mathbf{z}) \log \frac{p(\mathbf{x}|\mathbf{z})}{p(\mathbf{x})} d\mathbf{x}d\mathbf{z} . \qquad (15)$$

Given that our variables of interest are multivariate Gaussian distributions, the parameters of the marginal density $p(\mathbf{x})$ are trivially the Kalman prior mean $\mathbf{x}(t + \tau|t)$ and covariance $\Sigma(t+\tau|t)$. Moreover, the parameters of the conditional density $p(\mathbf{x}|\mathbf{z})$ come precisely from the Kalman update equations $\mathbf{x}(t + \tau|t + \tau)$ and $\Sigma(t + \tau|t + \tau)$. Substituting the general form of the Gaussian distribution in Eq. (15), we obtain the expression

$$\mathcal{I}(\mathbf{x}, \mathbf{z}) = \frac{1}{2} \left( \log |\Sigma(t + \tau|t)| - \log |\Sigma(t + \tau|t + \tau)| \right) . \quad (16)$$

Thus, in choosing a maximally mutually informative motion command, we are maximizing the difference between prior and posterior entropies [9]. In other words, we are choosing the motion command that most reduces the uncertainty of $\mathbf{x}$ due to the knowledge of $\mathbf{z}$. Observe however, that given our constant velocity model for the prior estimation of platform pose, base orientation changes will not alter the prior covariance $\Sigma(t + \tau|t)$. That is because the orientation change $\beta$ repercutes only in the location of the attach points in the base $\mathbf{a}_i$ and can not modify the constant Jacobians $F$ or $G$.

For this reason, for our particular system, when comparing the gain in Mutual Information induced by a set of motion commands, we need only to analyze the changes in posterior entropy

$$\mathcal{H}(\mathbf{x}|\mathbf{z}) = \frac{1}{2} \log |\Sigma(t + \tau|t + \tau)| \qquad (17)$$

and choose the action that minimizes it.

$$\beta^* = \operatorname{argmin}_{\beta \in U} |\Sigma(t + \tau|t + \tau)| \qquad (18)$$

The real-time requirements of the task preclude evaluating such metric for a large discrete set of actions within the range of possible commands. In our case, the set of actions evaluated at fixed values of $\beta$ are $U = \{\texttt{rotate-left}, \texttt{stop}, \texttt{rotate-right}\}$. The scheme is illustrated in Figure 3. Similar applications requiring real-time performance that use mutual information to base their actions have been repoorted in [10], [11].

## V. Preventing Wire Crossings

Providing the base with the ability to rotate has the added advantage of increasing the range of motion of the tracked platform; mainly, for rotations along the vertical axis. Special care must be taken however, to ensure that such base rotations
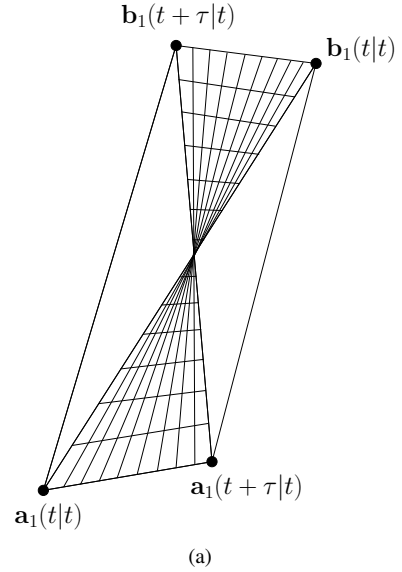


(a)

Fig. 4.    The tetrahedron defined by the prior and posterior estimates of the wire attach points at the base and the platform is a conex bound of the trajectory of such wire moving at constant velocity.

will not induce wire crossings. Considering that wire end-point displacements are sufficiently small per sampling interval, and that both the base and the platform move at constant velocity, the trajectory described by each wire can be assumed to be bounded by the tetrahedron described by the prior and posterior estimates of the wire attaching points at the base and the platform. One way to guarantee that such wire crossings will not occur is by checking whether these tetrahedra do not intersect each other. That is, we must verify that for the three wires, the tetrahedra described by the four attaching points $\{\mathbf{a}_i(t|t), \mathbf{a}_i(t + \tau|t), \mathbf{b}_i(t|t), \mathbf{b}_i(t + \tau|t)\}$ do not intersect.

A very fast test for tetrahedra intersection is based on the Separating Axis Theorem described in the computer graphics literature [12]. The test consists on checking whether the plane lying on the face of each tetrahedra separates the two of them. To implement this test, we need to compare the signed volume described by one of the tetrahedra to the signed volume of the four tetrahedra formed by joining the separating face with each of the vertices in the other tetrahedron. Figure 5 shows two possible trajectories for wires 1 and 2. When the face under scrutiny is $\{\mathbf{a}_2(t|t), \mathbf{a}_2(t + \tau|t), \mathbf{b}_2(t|t)\}$, and the trajectories do not intersect (see Fig. 5(a)), the following must hold

$$\begin{aligned} &\operatorname{sgn} \begin{vmatrix} \mathbf{a}_2(t|t) & \mathbf{a}_2(t + \tau|t) & \mathbf{b}_2(t|t) & \mathbf{a}_1(t|t) \\ 1 & 1 & 1 & 1 \end{vmatrix} \\ =\ &\operatorname{sgn} \begin{vmatrix} \mathbf{a}_2(t|t) & \mathbf{a}_2(t + \tau|t) & \mathbf{b}_2(t|t) & \mathbf{a}_1(t + \tau|t) \\ 1 & 1 & 1 & 1 \end{vmatrix} \\ =\ &\operatorname{sgn} \begin{vmatrix} \mathbf{a}_2(t|t) & \mathbf{a}_2(t + \tau|t) & \mathbf{b}_2(t|t) & \mathbf{b}_1(t|t) \\ 1 & 1 & 1 & 1 \end{vmatrix} \\ =\ &\operatorname{sgn} \begin{vmatrix} \mathbf{a}_2(t|t) & \mathbf{a}_2(t + \tau|t) & \mathbf{b}_2(t|t) & \mathbf{b}_1(t + \tau|t) \\ 1 & 1 & 1 & 1 \end{vmatrix} \\ \neq\ &\operatorname{sgn} \begin{vmatrix} \mathbf{a}_2(t|t) & \mathbf{a}_2(t + \tau|t) & \mathbf{b}_2(t|t) & \mathbf{b}_2(t + \tau|t) \\ 1 & 1 & 1 & 1 \end{vmatrix} \end{aligned} \quad (19)$$

However, when the plane on which the face $\{\mathbf{a}_2(t|t), \mathbf{a}_2(t+\tau|t), \mathbf{b}_2(t|t)\}$ lies is not a separating one (see Fig. 5(b)), then
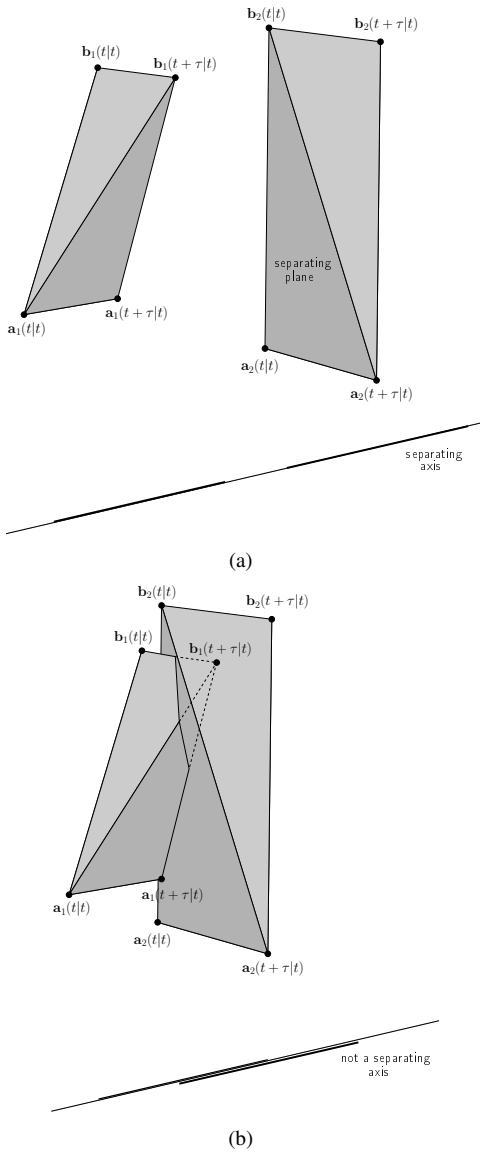
Fig. 5. To test for wire crossings the signed volumes for the tetrahedra formed by grouping the separating plane and each vertex of one of the tetrahedra must be of opposite sign to the volume of the other tertrahedron. (a) the tetrahedra do not intersect, (b) the tetrahedra intersect.

one (or all) of the vertices in the last row of the determinants in the left side of the inequality (19) will produce an opposite signed volume. If that is the case, the test must be exhausted for the two remaining faces of the tetrahedron; and if the search for a separating plane completes without success, then we can say that the proposed wire trajectories intersect, and must avoid the causing motion command.

## VI. IMPLEMENTATION AND EXAMPLES

### A. Mechanical Considerations of the Implemented Test-bed

In a cable extension transducer, commonly known as a string pot, the tension of the cable is guaranteed by a spring connected to its spool. Using a cable guide, the cable is allowed to move within a $20°$ cone, making it suitable for 3D motion applications. There are cable guides that permit $360°$ by $317°$ displacement cable orientation flexibility. Manufacturers of
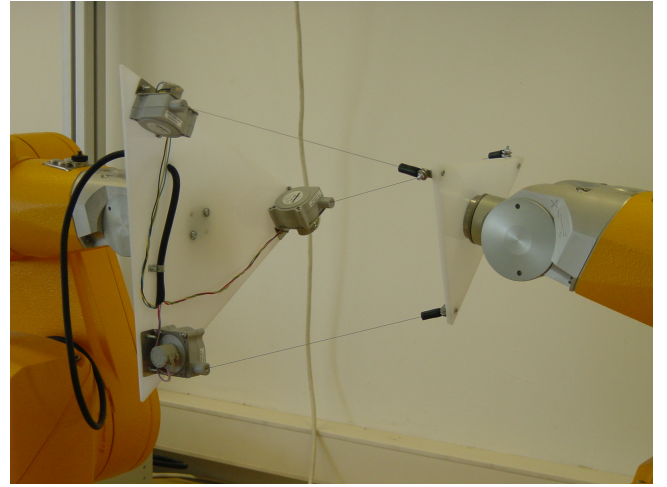
such sensors are Celesco Transducer Products Inc., SpaceAge Control Inc., Carlen Controls Inc., and several others.

String pots provide a long range $(0.04 - 40m)$, with typical accuracy of 0.02% of full scale. The maximum allowable cable velocity is about $7.2m/s$ and the maximum cable acceleration is about $200m/s^2$.

The usefulness of a tracking device depends on whether it can track the motion fast enough. This ability is determined by the lag, or latency, between the change of the position and orientation of the target being tracked and the report of the change to the computer. In virtual reality applications, lags above 50 milliseconds are perceptible to the user. In general, the lag for mechanical trackers is typically less than $5ms$.

The implemented system consists of a methacrylate triangular base with 0-50 inch SP1 Celesco string pots attached to its corners as shown in Fig. 6. The base is fixed on its center to a RX60 Staubli arm that induces rotation at desired values. The moving platform is made also of a triangular methacrylate piece holding the string pot end point attachments. This piece is mounted on a second Staubli arm so as to produce repeatible experiments in a measurable waw. Wire length measurements are read on a PC by means of an off-the-shelf National Instruments Data Acquisition Card.

The coordinates of the attaching points in both the base and the platform can be found in Tb. I, and refer to the frames shown in Figure 1.



Fig. 6. A testbed for the proposed 3-Wire Active Sensing Device

TABLE I
COORDINATES OF THE ATTACHING POINTS (IN METERS) IN THEIR LOCAL
COORDINATE FRAMES.

|        | $x$     | $y$     | $z$    |
|--------|---------|---------|--------|
| $a_1$  | 0.3000, | 0.0000, | 0.0000 |
| $a_2$  | -0.1500,| 0.2598, | 0.0000 |
| $a_3$  | -0.1500,| -0.2598,| 0.0000 |
| $b_1$  | 0.1000, | 0.0000, | 0.0000 |
| $b_2$  | -0.0500,| 0.0866, | 0.0000 |
| $b_3$  | -0.0500,| -0.0866,| 0.0000 |

*B. Maximum Base Rotation Speed*

The quality of the estimated pose is directly influenced by the velocity at which the base can rotate. To determine the range of motion velocities that can be tracked with our system, a tracking simulation was repeated limiting the base rotation velocity. A set of 20 runs was conducted, varying the maximum platform rotation speed from 0 to 1 $rad/s$, and with time steps of 0.01 $s$; the tracked object translating at a constant velocity of 0.2 $m/s$ along the $x$ axis, and rotating at $\frac{\pi}{10} rad/sec$ about an axis perpendicular to the base. The best pose estimations are achieved when the base rotates at twice the speed of the tracked object, approximately $\frac{\pi}{5} rad/s$ for this experiment.

*C. Pure rotations*

A second experiment consisted in testing the tracking system under pure rotations along the vertical axis. The idea is to show that, whenever cable crossing allows it, the largest motion commands are selected. This is because prior and posterior entropy difference is maximized for the largest possible configuration changes.

For this example, the object to be tracked rotated at $\frac{\pi}{10}$ $rad/s$, whilst kept at a distance of 1 $m$ from the base. The maximum base rotation speed was limited to $\frac{\pi}{5}$ $rad/s$. Figure 7(a) shows the evolution of the wire length measurements along the trajectory. Wire length sensors are modeled with additive Gaussian noise with zero mean and 1 $mm$ standard deviation. Figures 7(b) and 7(c) show the tracked object position and orientation recovery errors, respectively. The motion of the rotating base is depicted in Figure 7(d), showing that commands for maximal platform rotation velocities are being selected from our mutual information metric (Figure 7(e)).

*D. Compound motions*

In this last example, the tracked object moves back and forth in the three Cartesian components along a line from $(1, 1, 1)$ to $(2, 2, 2)$ meters, whilst rotating $\pi/3 rad$ about its center in all raw, pitch and yaw components. This experiment shows that for compound motions it is more difficult to disambiguate orientation error, while still doing a good job at tracking the correct object pose. Once more, the maximum base rotation speed was limited to $\frac{\pi}{5}$ $rad/sec$. Figure 8(a) shows the evolution of wire length measurements for this example. The tracked object position and orientation errors is shown in Figures 8(b) and 8(c). The motion of the rotating base is depicted in Figure 8(d). And, our mutual information action selection mechanism is shown in Figure 8(e).

## VII. Conclusion

An active sensing strategy for a wire tracking device has been presented. It has been shown how, by allowing the sensor platform rotate about its center, a wider range of motions can be tracked by reducing the number of wires needed from 6 to 3, combined with a typical state estimation scheme. Platform rotation commands are chosen so as to maximize the mutual
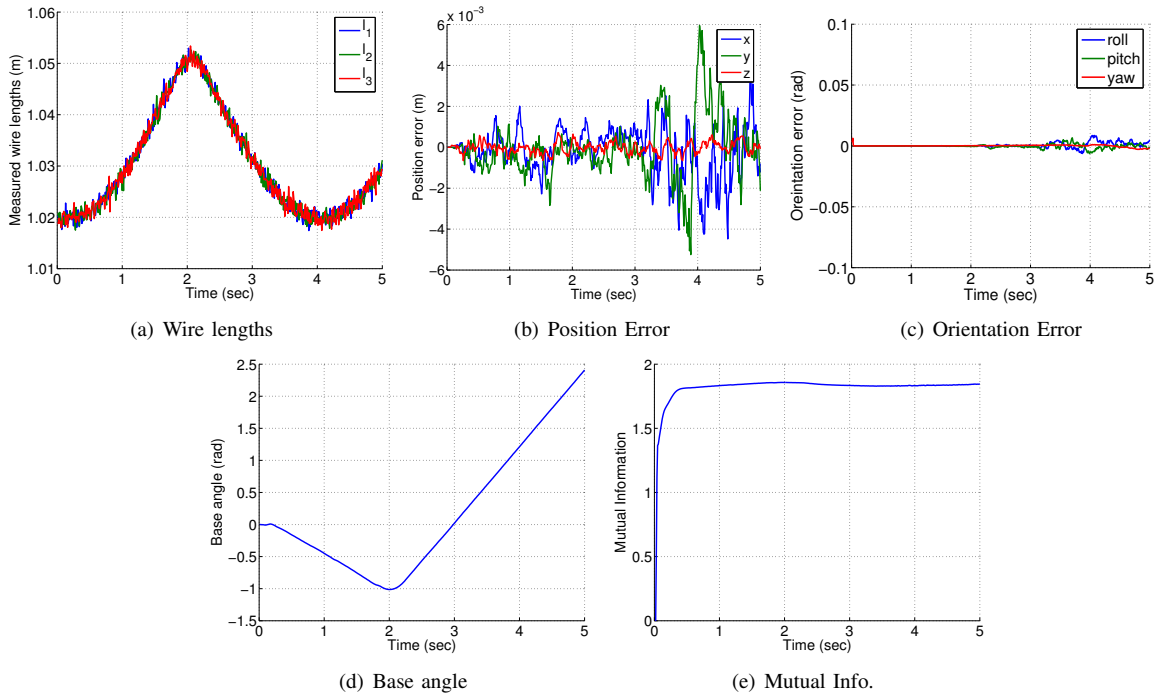
information between poses and measurements, which turns out in our case to be aquivalent to choosing those actions that most reduce state estimation entropy. A heuristic to prevent wire wrappings is also considered.

The feasibility of developing such a device has been shown with an implementation using a dual-Staubli-arm workbench. Our experiments suggest as a limitation of the approach that the rate of base rotation speed should be at least twice compared to platform speed.

## References

[1] Z. J. Geng and L. S. Haynes, "A 3-2-1 kinematic configuration of a Stewart platform and its application to six degree of freedom pose measurements," *Robot. Comput.-Integr. Manuf.*, vol. 11, no. 1, pp. 23–34, 1994.

[2] J. Jeong, S. Kim, , and Y. Kwak, "Kinematics and workspace analysis of a parallel wire mechanism for measuring a robot pose," *Mech. Mach. Theory*, vol. 34, no. 6, pp. 825–841, 1999.

[3] P. Nanua and K. Waldron, "Direct kinematics solution of a special parallel robot structure," in *Proc. 8th CISM-IFToMM Sym. Theory Practice Robot Manipulators*, Warsaw, 1990, pp. 134–142.

[4] K. Hunt and E. Primrose, "Assembly configurations of some in-parallel-actuated manipulators," *Mech. Mach. Theory*, vol. 28, no. 1, pp. 31–42, 1993.

[5] F. Thomas, E. Ottaviano, L. Ros, and M. Ceccarelli, "Performance analysis of a 3-2-1 pose estimation device," *IEEE Trans. Robot.*, vol. 21, no. 3, pp. 288–297, Jun. 2005.

[6] M. Griffis and J. Duffy, "A forward displacement analysis of a class of Stewart platforms," *J. Robot. Syst.*, vol. 6, no. 6, pp. 703–720, 1989.

[7] P. Nanua, K. Waldron, and V. Murthy, "Direct kinematic solution of a Stewart platform," *IEEE Trans. Robot. Automat.*, vol. 6, no. 4, pp. 438–444, 1990.

[8] V. Parenti-Castelli and C. Innocenti, "Direct displacement analysis for some classes of spatial parallel mechanisms," in *Proc. 8th CISM-IFToMM Sym. Theory Practice Robot Manipulators*, Warsaw, 1990, pp. 126–133.

[9] D. J. C. MacKay, "Information based objective functions for active data selection," *Neural Comput.*, vol. 4, no. 4, pp. 589–603, 1992.

[10] A. Davison, "Active search for real-time vision," in *Proc. IEEE Int. Conf. Comput. Vision*, Beijing, Oct. 2005, pp. 66–73.

[11] T. Vidal-Calleja, A. Davison, J. Andrade-Cetto, and D. Murray, "Active control for single camera SLAM," in *Proc. IEEE Int. Conf. Robot. Automat.*, Orlando, May 2006, pp. 1930–1936.

[12] F. Ganovelli, F. Ponchio, and C. Rocchini, "Fast tetrahedron-tetrahedron overlap algorithm," *ACM J. Graphics Tools*, vol. 7, no. 4, 2003.

[13] H. Bruynickx, "Forward kinematics for hunt-primrose parallel manipulators," *Mech. Mach. Theory*, vol. 34, pp. 657–664, 1999.

[14] J. P. Merlet, *Parallel Robots*, 2nd ed., ser. Solid Mechanics and its Applications. New York: Springer, 2006, vol. 128.

[15] V. Parenti-Castelli and R. Di Gregorio, "A new algorithm based on two extra-sensors for real-time computation of the actual configuration of the generalized stewart-gough manipulator," *J. Mech. Design*, vol. 122, no. 3, pp. 294–298, Sep. 2000.

[16] D. MacKay, *Information Theory, Inference, and Learning Algorithms*. Cambridge: Cambridge University Press, 2003.

(a) Wire lengths

(b) Position Error

(c) Orientation Error

(d) Base angle

(e) Mutual Info.

Fig. 7.   Wire tracking of pure rotations along an axis perpendicular to the base platform.



(a) Wire lengths
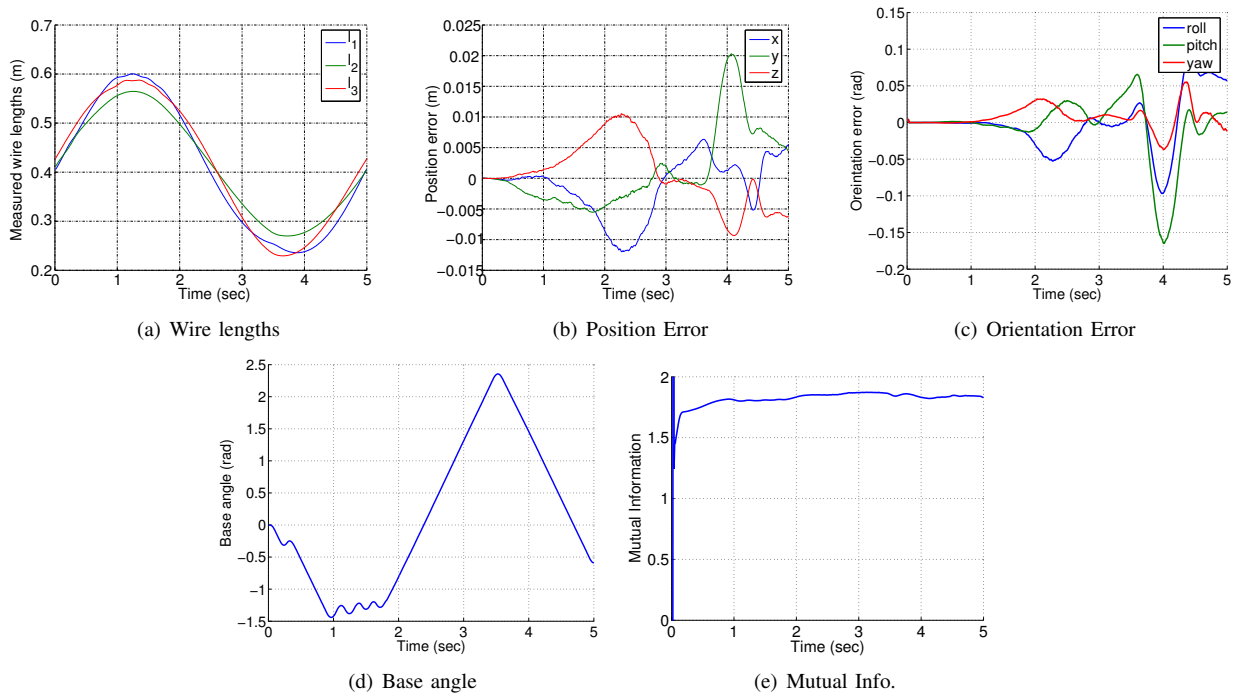
(b) Position Error

(c) Orientation Error

(d) Base angle

(e) Mutual Info.

Fig. 8.   Wire tracking of compound motion.